Proceedings of the
47th IEEE Conference on Decision and Control
Cancun, Mexico, Dec. 9-11, 2008

Multi-rate optimizing control of simulated moving beds

Cristian Grossmann, Christian Langel, Marco Mazzotti, Massimo Morbidelli, Manfred Morari

Abstract— **This paper presents an optimizing control scheme for simulated moving beds (SMB) that allows multi-rate (MR) sampled measurements to be incorporated into the control and estimation problem in a clear and transparent manner. This is particularly relevant for chiral separations where online monitoring requires the combination of various analytical techniques that may operate on widely varying time scales. An MR periodic linear time-varying (PLTV) model is derived for the SMB process. The cyclic nature of the process is exploited by formulating the MR PLTV model within a repetitive model predictive control framework. Simulation results for a chiral separation are presented. The proposed multi-rate controller is able to deliver increased productivity while respecting the process and product specifications.**

I. INTRODUCTION

Simulated Moving Bed (SMB) is a continuous chromatographic process used to separate into two fractions a mixture of molecules dissolved in a fluid phase. The separation principle is based on the different affinities of the molecules in the mixture to the solid-phase which moves countercurrently to the direction of the fluid. The SMB consists of a loop of n_{col} columns where the fluid circulates in one direction (Fig. 1). The desired countercurrent flow between the two phases is achieved by switching the inlet and outlet ports in the direction of the fluid flow every t^* seconds, which results in a *simulated* countercurrent movement of the solid with respect to the fluid. This periodic switching gives rise to a cyclic behavior of the process, which does not achieve a steady state with constant process variable profiles, but rather a cyclic steady state, where these profiles are repeated periodically. A detailed description of the process can be found elsewhere [1].

Economic advantages, like higher productivity and lower solvent consumption, have firmly established SMB in recent years as the state-of-the-art technology for complex separation tasks in the areas of pharmaceuticals, fine chemicals and biotechnology, especially for the purification of species characterized by low selectivities, i.e. difficult to separate, such as chiral molecules for single enantiomer drug development. Nevertheless, the full exploitation of the economic advantages of SMB has been hindered mainly by the uncertainty in physical properties of the mixture, i.e. its adsorption behavior on the solid phase, which is a limiting factor in the optimal design and operation of the SMB separations. Furthermore the determination of the adsorption behavior is by itself a very difficult and time-consuming task. These facts enforce the selection of conservative operating conditions that will guarantee the fulfillment of the strict purity requirements in the face of uncertainty, at the price of sacrificing productivity. The full economic potential of the SMB can be exploited by using a proper feedback control scheme. Several approaches have been proposed and a detailed review of these different control schemes may be found in the literature [3], [4]. In general, the bottleneck of these approaches is again, the need for accurate data about the adsorption behavior.

In the past years, the control group at ETH Zurich proposed and verified experimentally an SMB control scheme which guarantees the fulfillment of product and process specifications, such as minimum purities and maximum allowable pressure drop, while optimizing the economics of the process [3], [5]. It is noteworthy that this controller requires only minimal information on the adsorption behavior of the components to separate, i.e., only the linear adsorption isotherm, which can be determined experimentally in a straightforward and reliable manner.

Recently, multi-rate controllers and estimators have been presented in various areas, like polymerization processes [2]. This paper presents a multi-rate model predictive controller that combines optical detector signals with high performance liquid chromatography (HPLC) measurements, i.e. $'$fast$'$ and $'$slow$'$ sampled-data, in a systematic way. In this way, the $'$fast$'$ sampled-data allows one to follow the cyclic time evolution of the process, while the $'$slow$'$ sampled-data incorporates the information about the product quality.

This paper is structured as follows: Section II gives a brief description of the virtual SMB plant and monitoring techniques considered in this work. Section III explains in detail the development multi-rate SMB model and the control problem formulation. In section IV the effectiveness of this control approach is assessed and demonstrated through simulations on a virtual SMB unit for the separation of the guaifenesin enantiomers. Finally, conclusions are presented.

II. PROCESS DESCRIPTION

A. SMB Virtual Plant

A racemic mixture of the guaifenesin enantiomers (A and B) is to be separated in a four-section SMB unit with $n_{col} = 8$ columns arranged in a 2-2-2-2 configuration as shown in Fig. 1. The dynamical model for simulation of the SMB unit is obtained by interconnecting the dynamical models of each chromatographic column. The single-column dynamics are modelled with the equilibrium dispersive model (EDM) and the adsorption behavior of both components inside the columns is described by a linear adsorption isotherm, with

C.Grossmann and M.Morari belong to the Automatic Control Lab., C.Langel and M.Mazzotti belong to the Inst. of Process Engineering, M.Morbidelli belongs to the Inst. for Chem. and Bio-Engineering, ETH Zurich, 8092 Zurich, Switzerland.
morari@control.ee.ethz.ch

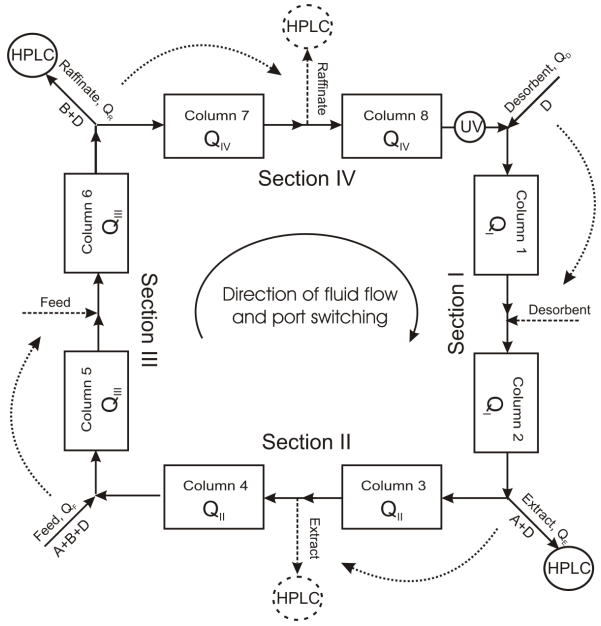

Fig. 1. Scheme of an SMB unit. The dashed lines indicate the inlet/outlet positions after the first switch. The primary, slow-sampled measurements are taken by the HPLC in the extract and raffinate ports. The secondary, fast-sampled measurements are recorded by the UV absorbance detector.

Henry's constants H_A and H_B. The mathematical model is completed by considering the corresponding node balances between the columns and the proper boundary and initial conditions. The parameters of the system under consideration are reported in section IV.

B. Concentration determination of chiral mixtures

Enantiomers have the same chemical and physical properties, except for their rotation of polarized light and their behavior in chiral environments. This makes the pool of available analytical methods to determine the concentrations of both enantiomers in a mixture rather limited.

1) Optical detectors: Through a combination of a UV absorbance detector and a polarimeter the concentrations of a pair of enantiomers in the stream j, $c_{A,j}(t)$ and $c_{B,j}(t)$ can be determined at a given time t. Commercial UV absorbance detectors give very accurate and reliable measurements, whereas the limiting factor in this approach is the very low accuracy of today's commercially available polarimeters for this kind of applications. Since performance of the controller will greatly depend on the precision and accuracy of the analytical methods it relies on to get the feedback information, we refrain from the use of polarimeters in this control approach to avoid a deterioration in the performance. As a result the fast sampled-data from the UV absorbance detector will render only the *sum* of the concentrations of A and B.

$$S_{UV,j}(t) = k_{UV}(c_{A,j}(t) + c_{B,j}(t)) \tag{1}$$

where $S_{UV,j}$ is the signal read form the UV detector and k_{UV} is the calibration factor. The UV detector is placed at the end of column 8, i.e. $j = 8$, as depicted in Fig. 1.

2) HPLC measurements: It is possible to collect samples of the mixture over a period of time τ and analyze them with an HPLC system. These measurements will deliver the *average* concentrations of both species, $c^{ave}_{A,j,\tau}$ and $c^{ave}_{B,j,\tau}$, in the stream j over the period of time τ

$$c^{ave}_{i,j,\tau} = \frac{\int_0^\tau c_{i,j}(t)Q_j(t)dt}{\int_0^\tau Q_j(t)dt} \tag{2}$$

for $i = A, B$. The factor $Q_j(t)$ is the flow rate of stream j, from which the sample was collected. As in the 'cycle to cycle' controller [5], we collect samples of the extract and raffinate streams $j = E, R$, over a period of time $\tau = n_{col}\, t^*$, the cycle time. The HPLC measurements are therefore taken at rather low frequencies. As mentioned earlier, HPLC technology is well established and so these measurements are highly accurate and reliable.

In this work we present a framework to systematically combine fast- and slow-sampled measurements. In this way, it is possible to combine the two most accurate methods for chiral concentration determination, UV absorbance detectors and HPLC measurements.

III. MULTI-RATE MPC

A. Control concept

The core of the control concept is the integration of the optimization and control of the SMB unit [3]. The novel feature presented in this work is the extension of the $'$cycle to cycle$'$ control concept that uses the low frequency sampled data as feedback information, to incorporate the high frequency UV signal as secondary measurements [5]. A scheme of the control concept is shown in Fig. 2.

The control problem is formulated as a constrained dynamic

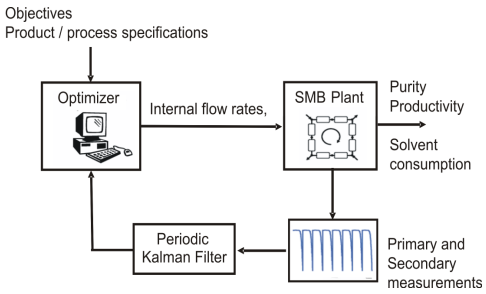

Fig. 2. Scheme of the multi-rate control concept.

optimization problem within the repetitive MPC (RMPC) framework [6]. The productivity and solvent consumption represent the cost function to be optimized, while the hardware restrictions and product quality specifications are imposed as constraints. The controller makes use of a simplified periodically linear time-varying (PLTV) SMB model to predict and optimize the performance of the unit over a predefined number of cycles, the so-called prediction horizon, n_p. The simplified PLTV SMB model requires only the linear isotherm information, H_A and H_B, about the mixture to be separated. This scheme is implemented according to a receding horizon strategy. The states are estimated using

a periodic Kalman filter. The measurements, optimization and control actions are performed N times within a cycle. In this approach the switch time t^* is fixed *a priori*. The internal flow rates in the four sections of the unit, Q_I, Q_{II}, Q_{III}, Q_{IV}, are used as manipulated variables. The primary measurements are the concentration levels in the extract (E) and raffinate (R) streams averaged over one cycle, $c^{ave}_{A,E}$, $c^{ave}_{B,E}$, $c^{ave}_{A,R}$, $c^{ave}_{B,R}$. The secondary measurement is the sum of the concentrations of the enantiomers recorded by the UV detector fixed at the outlet of column 8, i.e. $(c_{A,8}(t) + c_{B,8}(t))$.

B. Modeling

The key idea here is to develop a reduced-order PLTV model for estimation and control purposes starting from the first principles, hybrid nonlinear model. Since standard model reduction techniques have been developed for linear time-*invariant* (LTI) systems, we first transform, or lift, the full-order PLTV model into an LTI model to apply a balanced model reduction. We then unlift the reduced-order LTI model to get the desired reduced-order PLTV and incorporate it into the RMPC formulation. The simplification procedure follows the same steps as presented in [5] and [6] and extends it for multi-rate systems along the lines presented in [7].

1) First principles, hybrid nonlinear model: The SMB unit can be described by first principles models. These models are systems of partial differential equations (PDEs), describing the behavior of the two enantiomers inside each chromatographic column as a function of position, z, and time, t. To complete the mathematical model, the PDEs are combined with algebraic equations (AEs) that account for the node balances. Note that every t^* seconds, the input/output ports are switched and the configuration of the unit changes, giving rise to a new system of PDEs and AEs that describe the dynamics of the SMB unit. The simplification procedure starts by discretizing the space coordinate z in $n_g \cdot n_{col}$ grid points. The n_{col} systems of PDEs and AEs can then be simplified to n_{col} systems of nonlinear ordinary differential equations (ODEs). An SMB unit with $n_{col} = 8$ columns separating $n_s = 2$ species and discretized in $n_g = 40$ grid points per column, gives rise to n_{col} systems of ODEs of $n_{eq} = n_g \cdot n_s \cdot n_{col} = 640$ equations each. Each system of ODEs can be recast in the following form

$$\begin{aligned} \frac{d\mathbf{c}}{dt} &= \mathbf{f}^p(\mathbf{c}, \mathbf{Q}) \\ \mathbf{c}_{out} &= \mathbf{g}^p_{out}(\mathbf{c}) \\ \mathbf{c}_{uv} &= \mathbf{g}^p_{uv}(\mathbf{c}) \qquad p = 1, \ldots, n_{col} \end{aligned} \tag{3}$$

Here, the index p denotes the number of different input/output port configurations of the SMB unit. The vector $\mathbf{Q}$ comprises the internal flow rates in the four sections, i.e., $Q_I, \ldots, Q_{IV}$, and $\mathbf{c}$ is the state vector containing the internal concentration values along each column h, i.e., $\bar{c}_{i,h,g}(t)$ for $i = A, B$, $h = 1, \ldots, n_{col}$ and $g = 1, \ldots, n_g$. The primary measurements $\mathbf{c}_{out}$ are the concentration levels of the two enantiomers in the raffinate and extract outlets streams, i.e., $c_{A,R}(t)$, $c_{B,R}(t)$, $c_{A,E}(t)$, $c_{B,E}(t)$, where the samples will be collected over one cycle to compute the average concentrations according to (2). The secondary measurements $\mathbf{c}_{uv}$ is the signal recorded from the UV absorbance detector.

2) Multi-rate linear model: The ODE systems in (3) are linearized and subsequently discretized in time. For details on how to choose the linearization point please refer to [5]. The resulting discrete time, state-space, PLTV SMB model has the following structure

$$\begin{aligned} x_k(n+1) &= A(n)x_k(n) + B(n)u_k(n) \\ y^c_k(n) &= C^c(n)x_k(n) \\ y^s_k(n) &= C^s(n)x_k(n) \\ &\text{for} \quad n = 0, \ldots, N-1 \\ x \in \mathbf{R}^{n_{eq}},\ u \in \mathbf{R}^{n_u},\ y^c &\in \mathbf{R}^{n_{y^c}},\ y^s \in \mathbf{R}^{n_{y^s}} \end{aligned} \tag{4}$$

The variables x and u are the state and input vectors comprising the internal concentration profiles and the internal flow rates, respectively. y^c and y^s are the primary and secondary outputs, respectively. The state, input and output vectors are defined in terms of deviation variables with respect to the reference cyclic steady state profiles used for linearization [3]. Here, k is the cycle index and n is the time index running within the cycle; N is the number of time steps within a cycle used for time discretization. In the equations above, $n_{y^c} = 4$, $n_{y^s} = 1$ and $n_u = 4$ are the number of primary and secondary measurements and manipulated variables, respectively. For the transition from one cycle to the next, we impose the continuity requirement

$$x_{k+1}(0) = x_k(N) \tag{5}$$

The output $y^c_k(n)$ of the PLTV model in (4) describes the instantaneous concentrations of both components in the two outlet streams for each time step n within the cycle k. Nevertheless, the primary measurements will be the concentration of both species in extract and raffinate *averaged over one cycle*. Therefore, the PLTV model has to be modified such that the required average concentrations are directly given by the primary model output, i.e. a $'$cycle to cycle$'$ SMB model. For this purpose, the model in (4) is lifted, i.e. successively substituted for the time steps $n = 0, \ldots, N-1$. The $'$cycle to cycle$'$ SMB model providing the average concentrations for one cycle as primary output and *all* secondary measurements of cycle k as secondary outputs can be cast as

$$\begin{aligned} x_{k+1}(0) &= \mathbf{\Phi}x_k(0) + \mathbf{\Gamma}\mathbf{U}_k \\ \mathbf{Y}^{c,ave}_k &= \mathbf{\Pi}^c x_k(0) + \mathbf{G}^c\mathbf{U}_k \\ \mathbf{Y}^s_k &= \mathbf{\Pi}^s x_k(0) + \mathbf{G}^s\mathbf{U}_k \\ \mathbf{U} \in \mathbf{R}^{(N\times n_u)},\ \mathbf{Y}^{c,ave} &\in \mathbf{R}^{n_{y^c}},\ \mathbf{Y}^s \in \mathbf{R}^{(N\times n_{y^s})} \end{aligned} \tag{6}$$

For the sake of space, please refer to [5] for the details on the construction of the state space matrices. The inputs, primary and secondary outputs of one cycle have been grouped as

$$\begin{aligned} \mathbf{U}_k &= \begin{bmatrix} u^T_k(0) & \cdots & u^T_k(N-1) \end{bmatrix}^T \\ \mathbf{Y}^{c,ave}_k &= \begin{bmatrix} y^{c,ave}_{A,E,k} & y^{c,ave}_{B,E,k} & y^{c,ave}_{A,R,k} & y^{c,ave}_{B,R,k} \end{bmatrix}^T \\ \mathbf{Y}^s_k &= \begin{bmatrix} {y^s_k}^T(0) & \cdots & {y^s_k}^T(N-1) \end{bmatrix}^T \end{aligned} \tag{7}$$

3) Repetitive Model predictive control formulation: So far, a multi-rate ′cycle to cycle′ SMB model has been developed. In this section it is reformulated within the RMPC framework [6]. A brief explanation of the unlifting procedure to obtain now a reduced order PLTV model is given below. A more detailed description can be found in [3].

The resultant lifted model in (6) can be used to develop a feedback formulation, that utilizes the secondary measurements as they become available. For a more efficient online implementation, the order of the model is first reduced via balanced model reduction from $n_{eq} = 640$ to $\tilde{n}_{eq} = 26$ states. In the following, the superscript $(\cdot)$ stands for both primary, *(c,ave)*, and secondary measurements, *(s)*. Notice that once the cycle-to-cycle description in (6) has been reduced, it can be expressed in terms of incremental changes by differencing the model for two successive cycles as follows

$$\begin{aligned} \Delta\tilde{x}_{k+1}(0) &= \tilde{\mathbf{\Phi}}\Delta\tilde{x}_k(0) + \tilde{\mathbf{\Gamma}}\Delta\mathbf{U}_k \\ \bar{\mathbf{Y}}_k^{(\cdot)} &= \bar{\mathbf{Y}}_{k-1}^{(\cdot)} + \tilde{\mathbf{\Pi}}^{(\cdot)}\Delta\tilde{x}_k(0) + \mathbf{G}^{(\cdot)}\Delta\mathbf{U}_k \end{aligned} \tag{8}$$

where $\tilde{x}$ is the state vector of the reduced-order ′cycle to cycle′ SMB model with $\tilde{n}_{eq}$ states. The matrices $\tilde{\mathbf{\Phi}}$, $\tilde{\mathbf{\Gamma}}$, $\tilde{\mathbf{\Pi}}^{(\cdot)}$ and $\mathbf{G}^{(\cdot)}$ are the corresponding state-space matrices of appropriate dimensions. Here, Δ indicates the backwards difference with respect to the cycle index, e.g., $\Delta\mathbf{U}_k = \mathbf{U}_k - \mathbf{U}_{k-1}$ and $\Delta\tilde{x}_k(0) = \tilde{x}_k(0) - \tilde{x}_{k-1}(0)$. To unlift the model let us define

$$\begin{aligned} \delta_k(n) &\triangleq \Delta\tilde{x}_{k+1}(0) \\ \bar{\mathbf{y}}_k^{c,ave}(n) &\triangleq \bar{\mathbf{Y}}_k^{c,ave} \\ \bar{\mathbf{y}}_k^{s}(n) &\triangleq \bar{\mathbf{Y}}_k^{s}, \\ \text{with} \quad \Delta u_k(j) &= 0 \quad \text{for} \quad j \geq n \end{aligned} \tag{9}$$

This implies that the same input as for cycle $k-1$ is implemented starting at time n of the cycle k. Using these definitions, (8) can be rewritten as

$$\begin{aligned} \delta_k(n) &= \tilde{\mathbf{\Phi}}\Delta\tilde{x}_k(0) \\ &+ \left[\tilde{\mathbf{\Gamma}}_0 \cdots \tilde{\mathbf{\Gamma}}_{n-1}\right]\left[\Delta u_k^T(0) \cdots \Delta u_k^T(n-1)\right]^T \\ \bar{\mathbf{y}}_k^{(\cdot)}(n) &= \bar{\mathbf{Y}}_{k-1}^{(\cdot)} + \tilde{\mathbf{\Pi}}^{(\cdot)}\Delta\tilde{x}_k(0) \\ &+ \left[\mathbf{G}_0^{(\cdot)} \cdots \mathbf{G}_{n-1}^{(\cdot)}\right]\left[\Delta u_k^T(0) \cdots \Delta u_k^T(n-1)\right]^T \end{aligned} \tag{10}$$

where $\tilde{\mathbf{\Gamma}}_n$ and $\mathbf{G}_n^{(\cdot)}$ are the nth columns of the matrices $\tilde{\mathbf{\Gamma}}$ and $\mathbf{G}^{(\cdot)}$, respectively, corresponding to the input at time n. Note that $\delta_k(N) = \Delta\tilde{x}_{k+1}(0)$, $\bar{\mathbf{y}}_k^{c,ave}(N) = \bar{\mathbf{Y}}_k^{c,ave}$ and $\bar{\mathbf{y}}_k^{s}(N) = \bar{\mathbf{Y}}_k^{s}$ by definition (9). The model in (10) can be written for two consecutive time steps, i.e., for time n and $n+1$, and taking the difference, one obtains

$$\underbrace{\begin{bmatrix} \delta_k(n+1) \\ \bar{\mathbf{y}}_k^{c,ave}(n+1) \\ \bar{\mathbf{y}}_k^{s}(n+1) \end{bmatrix}}_{\bar{z}_k(n+1)} = \underbrace{I}_{\bar{A}} \underbrace{\begin{bmatrix} \delta_k(n) \\ \bar{\mathbf{y}}_k^{c,ave}(n) \\ \bar{\mathbf{y}}_k^{s}(n) \end{bmatrix}}_{\bar{z}_k(n)} + \underbrace{\begin{bmatrix} \tilde{\mathbf{\Gamma}}_n \\ \mathbf{G}_n^{c} \\ \mathbf{G}_n^{s} \end{bmatrix}}_{\bar{B}(n)} \Delta u_k(n) \tag{11}$$

The outputs can then be expressed as

$$\begin{aligned} \mathbf{y}_k(n) &= \underbrace{\begin{bmatrix} 0 & H^c(n) & 0 \\ 0 & 0 & H^s(n) \end{bmatrix}}_{\bar{C}(n)} \underbrace{\begin{bmatrix} \delta_k(n) \\ \bar{\mathbf{y}}_k^{c,ave}(n) \\ \bar{\mathbf{y}}_k^{s}(n) \end{bmatrix}}_{\bar{z}_k(n)} \\ H^c(n) &= I \qquad \text{for } n = 0 \\ H^c(n) &= \mathbf{0} \qquad \text{for } n = 1, \ldots, N-1 \\ H^s(n) &= \begin{bmatrix} \underbrace{0}_{n_{y^s} \times n \cdot n_{y^s}} & \underbrace{I}_{n_{y^s} \times n_{y^s}} & \underbrace{0}_{n_{y^s} \times (N-1-n) \cdot n_{y^s}} \end{bmatrix} \end{aligned} \tag{12}$$

Note that the output vector $\mathbf{y}$ comprises the primary and secondary process outputs at time n. The primary measurements though, are available only at the beginning of the cycle, i.e. $n = 0$. The transition from cycle-to-cycle completes the time-varying description of the system.

$$\underbrace{\begin{bmatrix} \delta_{k+1}(0) \\ \bar{\mathbf{y}}_{k+1}^{c,ave}(0) \\ \bar{\mathbf{y}}_{k+1}^{s}(0) \end{bmatrix}}_{\bar{z}_{k+1}(0)} = \underbrace{\begin{bmatrix} \tilde{\mathbf{\Phi}} & 0 & 0 \\ \tilde{\mathbf{\Pi}}^c & I & 0 \\ \tilde{\mathbf{\Pi}}^s & 0 & I \end{bmatrix}}_{\bar{\Psi}} \underbrace{\begin{bmatrix} \delta_k(N) \\ \bar{\mathbf{y}}_k^{c,ave}(N) \\ \bar{\mathbf{y}}_k^{s}(N) \end{bmatrix}}_{\bar{z}_k(N)} \tag{13}$$

The disturbances of the process are modelled as a stochastic difference equation capturing the effect of model errors and periodic disturbances that repeat themselves from cycle to cycle and the effect of random disturbances. The PLTV model in (11) - (13) can be written in the following compact form

$$\begin{aligned} \bar{z}_k(n+1) &= \bar{A}\bar{z}_k(n) + \bar{B}(n)\Delta u_k(n) \\ \mathbf{y}_k(n) &= \bar{C}(n)\bar{z}_k(n) \quad \text{for} \quad n = 0, \ldots, N-1 \\ \bar{z}_{k+1}(0) &= \bar{\Psi}\bar{z}_k(N) \end{aligned} \tag{14}$$

which constitutes the basis for the formulation of the state estimation filter presented next.

4) Time-varying periodic Kalman filtering: A periodically time-varying Kalman filter is found to be best suited for a recursive correction of the model errors by combining the model estimation and the available measurements. The one-step-ahead correction for the time-varying system in (14) is given by

$$\begin{aligned} \bar{z}_k(n+1|n) &= \bar{A}\bar{z}_k(n|n-1) + \bar{B}(n)\Delta u_k(n) \\ &+ K_k(n)\left[\mathbf{y}_k^{meas}(n) - \bar{C}(n)\bar{z}_k(n|n-1)\right] \\ \bar{z}_{k+1}(0|-1) &= \bar{\Psi}\bar{z}_k(N|N-1) \qquad n = 0, \ldots, N-1 \end{aligned} \tag{15}$$

where $\bar{z}_k(n+1|n)$ denotes the prediction of $\bar{z}_k(n+1)$ based on measurements available up to time n. $K_k(n)$ is the periodic time-varying Kalman filter gain matrix. Given the covariance matrices R_v and R_w of the white noise sequences v_k and w_k, respectively; a periodic time varying filter gain $K_k(n)$ and covariance matrix of the estimate $P_k(n)$, can be computed as in [3]. Instead of using $K_k(n)$ and $P_k(n)$, at each time step, one can, a priori iterate on the periodically time-varying Riccati difference until it converges to a periodic "steady-state" solution, i.e., $P_k(n) \longrightarrow P_\infty(n)$ and obtain the periodic steady-state gain matrices, i.e., $K_\infty(0), \cdots, K_\infty(N-1)$.

C. Optimization Problem

The controller has two main tasks. First, it should fulfill the product specifications while respecting the process constraints. Second, the controller should optimize the performance of the unit with respect to a given economic criterion. These tasks can be cast as a linear program (LP), which will be described in this section. The main idea is to incorporate the product specifications and process limitations as constraints in the LP, while the economic criteria represent the objective function for the optimization problem. Furthermore the system dynamics are included as equality constraints of the LP for numerical efficiency [8]. Each one of these points is discussed and presented in the following.

1) System Dynamics - Prediction: It is well known, that it is numerically efficient to have the input and state vectors of *every time step* of the prediction horizon as decision variables of the LP and include the system dynamics as equality constraints [8]. When following the modelling approach presented in the previous section, one faces a challenging trade-off when including the system dynamics into the LP as equality constraints:
On the one hand, in order to have a "good" prediction with high time resolution, one would need a rather fine time griding during one cycle, i.e. a large number N of grid points in time, which would result in large matrices build from the PLTV model in (14). The number of time grid points per cycle, N, generally lies in the order of 10^2, in our specific case, it was chosen to be $N = 64$.
On the other hand, the SMB process exhibits slow dynamics, which forces one to select rather long prediction horizons, generally, in the range of six to eight *cycles*, to have "good" predictions. Therefore the total number of time steps one would have to look into the future using model (14) to cover, for instance, six cycles, would be, $n_p = 6 \cdot 64 = 384$. Furthermore, recall that the number of states of the model considered in (14) is 94 and we have 4 inputs. The LP would consist of at least $(94+4) \cdot 384 = 37'632$ decision variables. In the following, we show how the number of decision variables was reduced by one order of magnitude by considering a reformulation of the multi-rate model developed in the previous section.
The model in (14) is a PLTV model that maps the state $\bar{z}_k(n)$ into the next $time\ step$ of the same cycle k, $\bar{z}_k(n+1)$. The key idea here, is to transform the PLTV model in (14), which maps the states from *time step to time step*, into a PLTV model that maps the states from *'cycle to cycle'*, i.e. that maps the state $\bar{z}_k(n)$ into $\bar{z}_{k+1}(n)$. To do so, starting at every time step $n = 0, ..., N-1$ we lift the model for one cycle. Note that this procedure had already been discussed when transforming the PLTV model in (4) into the 'cycle to cycle' model in (6), nevertheless, there it had been applied only for one time step, namely for $n = 0$, mapping $x_k(0)$ into $x_{k+1}(0)$. Now we do the same for every time step n. This yields N 'cycle to cycle' models, each one mapping the state at time step n of cycle k into the time step n of cycle $k+1$. This PLTV 'cycle to cycle' SMB model can be cast in the following compact form

$$\begin{aligned} \bar{z}_{k+1}(n) &= \mathcal{A}\bar{z}_k(n) + \mathcal{B}(n)\Delta\mathbf{U}_k(n) \\ \mathcal{Y}_k(n) &= \mathcal{C}(n)\bar{z}_k(n) + \mathcal{D}(n)\Delta\mathbf{U}_k(n) \\ \text{for} \quad n = 0, \dots, N-1 & \qquad \mathcal{Y} \in \mathbf{R}^{n_{y^s} \cdot N + n_{y^c}} \end{aligned} \tag{16}$$

These state-space matrices can be constructed through simple successive substitution of the models in (14). Note that the matrix $\mathcal{A}$ is not time dependent. From (14) we see that $\bar{A} = I$ for all n, except for the cycle transition equation, therefore $\mathcal{A} = \bar{\Psi}$. The inputs and outputs of the PLTV 'cycle to cycle' SMB model are defined as

$$\begin{aligned} \mathcal{Y}_k(n) &= \left[y_k^T(n) \dots y_l^T(i) \dots y_{k+1}^T(n-1)\right]^T \\ \Delta\mathbf{U}_k(n) &= \left[\Delta u_k^T(n) \dots \Delta u_l^T(i) \dots \Delta u_{k+1}^T(n-1)\right]^T \\ & \quad \text{where} \quad i = n, n+1, \dots N-1, 0, 1, \dots n-1 \end{aligned} \tag{17}$$

the cycle index $l = k$ if $n \leq i \leq N-1$ and $l = k+1$ if $0 \leq i \leq n-1$.
This model is incorporated into the optimization problem solved at time step n. For each time step n a set of equality constraints with the corresponding PLTV 'cycle to cycle' SMB model can be written over the prediction horizon to incorporate the system dynamics. In this way, the initial number of decision variables that would have been needed with the model in (14) of $37'632$ has been reduced to only $(94+256) \cdot 6 = 2100$, using the formulation in (16).

2) Product specifications and process limitations: The product is required to have a minimum purity. The average purity of the outlet stream $j = E, R$ over one cycle is defined as

$$P_{E,k}^{ave} = \frac{c_{A,E,k}^{ave}}{c_{A,E,k}^{ave} + c_{B,E,k}^{ave}}, \quad P_{R,k}^{ave} = \frac{c_{B,R,k}^{ave}}{c_{A,R,k}^{ave} + c_{B,R,k}^{ave}} \tag{18}$$

where each one of the average concentrations can be computed with Eq. (2). The purities in (18) is a nonlinear function of the concentration and flow rates and has to be linearized to be compatible with the LP formulation. The constraints for minimum purity over the prediction horizon n_p, can then be formulated as

$$P_{E,l}^{ave} \geq P_E^{min} - s_1 \qquad \text{with} \qquad s_1 \geq 0 \tag{19}$$

$$P_{R,l}^{ave} \geq P_R^{min} - s_2 \qquad \text{with} \qquad s_2 \geq 0 \tag{20}$$

$$\text{for} \qquad l = k+1, \dots, k+n_p$$

where s_1 and s_2 are slack variables to soften the constraints and avoid infeasibility problems. To account for the process limitations, the manipulated variables, are constrained during the whole operation with lower and upper bounds.

$$Q_j^{max} \geq Q_j \geq Q_j^{min} \quad \text{for} \quad j = I, \dots, IV \tag{21}$$

3) Cost function: The cost function of the LP is defined to maximize the productivity, in this case, by maximizing the feed flow rate Q_F and to minimize the desorbent consumption Q_D over a given prediction horizon n_p starting at

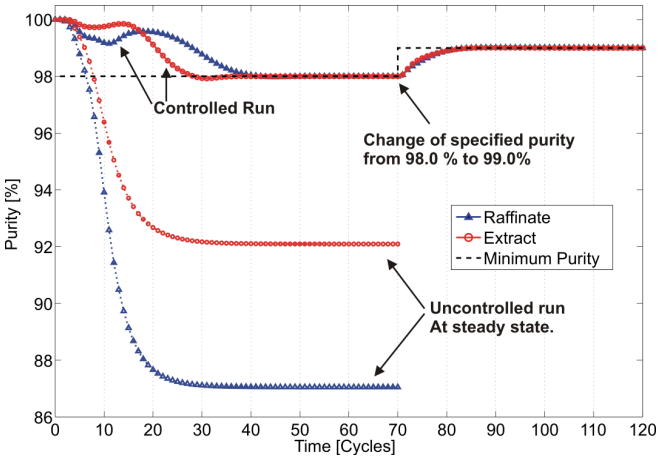

Fig. 3. Outlet purities vs time measured in cycles (1 cycle = $n_{col}t^*$ = 11.7 min). The dotted lines indicate a uncontrolled run under the starting conditions.

time step n of cycle k.

$$\min_{\Delta \mathbf{U}_k^{(n_p)}(n),\, \bar{Z}_k^{(n_p)}(n)} \left[\lambda_D \underbrace{Q_D^{(n_p)}}_{Q_I - Q_{IV}} - \lambda_F \underbrace{Q_F^{(n_p)}}_{Q_{III} - Q_{II}} \right] + \lambda_s \mathbf{s} \tag{22}$$

where $Q_D^{(n_p)}$ and $Q_F^{(n_p)}$ are the cumulative solvent consumption and feed throughput, respectively, over the prediction horizon n_p. The weighting factors λ_D, λ_F and λ_s reflect the relative preference given to the desorbent consumption minimization, the feed throughput maximization and the softening of the purity constraints, respectively. $\Delta \mathbf{U}_k^{(n_p)}(n)$ and $\bar{Z}_k^{(n_p)}(n)$ are the manipulated variables and states, respectively, for the prediction horizon n_p, at time step n of cycle k.

The set of inequalities in (19) - (21) and equality constraints in (16) complete the formulation of the LP, which comprised 2200 variables, 10800 inequality and 3100 equality constraints. A commercial solver, ILOG CPLEX 9.0 was used to solve the LP. The maximum computation time was found to be less than 0.6 s in a PC with a 2.4 GHz Intel Core 2 Quad processor.

IV. SIMULATION RESULTS

In the following example a startup scenario with changing specifications is presented to illustrate the performance of the multi-rate controller to fulfill the specified minimum purities by manipulating the four sectional flow rates.

The adsorption behavior of the chiral mixture to be separated can be described by a linear isotherm with Henry's constants $H_A = 1.25$ and $H_B = 0.61$, which are used for the model in the controller as well. The plant was started up at the reference flow rate ratios with initially clean columns and the controller was switched on at cycle 1. The parameters used in the cost function are $\lambda_F = 0.825$, $\lambda_D = 0.2$ and $\lambda_s = 1000$ to stress the fact, that the purity constraints should be softened to the least possible extent. Note that no control action at the startup conditions leads to very low purities as shown in the uncontrolled run in Fig. 3. The controller does not allow the purities to drop below the minimum specified purities of 98.0% at the startup and tracks them within 40 cycles. At cycle 70 the specifications are changed to 99.0% and the controller increases both purities within 15 cycles.

V. CONCLUSIONS AND FUTURE WORKS

In this study, an extension of the control concept developed earlier [3], [5] has been presented. This extension allows the controller to make use of multi-rate sampled-measurements, i.e. primary HPLC measurements and secondary UV absorbance measurements to control and optimize the unit.

A multi-rate periodic linear time-varying (MR-PLTV) model for the SMB process was developed in order to handle in a clean and systematic way the multi-rate sampled-measurements. The MR-PLTV was incorporated into the repetitive MPC framework to better exploit the cyclic nature of the process. Two different formulations of the MR-PLTV model were presented. The first formulation was for estimation purposes, which maps the states from *time step to time step*, thus providing the necessary information to design a PLTV Kalman filter. Nevertheless, this first formulation was not appropriate for predictive control due to the large number of time steps within a cycle, which on top of the slow SMB dynamics that require long prediction horizons, results in a prohibitively large control problem. The model was then reformulated into a MR-PLTV model that maps the states from *cycle to cycle*. This allowed the dynamics of the system to be efficiently incorporated into the optimization problem. The numerical example shows that the controller can assure the product quality and maximize the productivity, since the purities are at their lower bounds.

The future work aims at assessing and comparing this approach with the previous control formulations. Finally, this controller approach will be implemented and validated on our SMB pilot plant. This framework could be useful for other continuous cyclic chemical processes.

REFERENCES

[1] M. Mazzotti, G. Storti, and M. Morbidelli, Optimal operation of simulated moving bed units for nonlinear chromatographic separations, *J. of Chromatography A*, vol. 769, 1997, pp 3-24.

[2] M.T. Dokucu, M. Park, F.J. Doyle III, Multi-rate model predictive control of particle size distributions in a semibatch emulsion copolymerization reactor, *J. of Process Control*, vol. 18, 2008, pp 105-120.

[3] G. Erdem, S. Abel, M. Morari, M. Mazzotti, M. Morbidelli, and J. H.Lee, Automatic Control of Simulated Moving Beds, *Industrial and Engineering Chemistry Research*, vol. 43(2), 2004, pp 405-421.

[4] S. Engell, Feedback control for optimal process operation, *J. Process Control*, 17 (3), 2007, pp 203-219.

[5] C. Grossmann, M. Amanullah, G. Erdem, and M. Morari, and M. Mazzotti, and M. Morbidelli, Cycle to cycle optimizing control of simulated moving beds, *AIChE J.*, vol. 54, 2008, pp 194-208.

[6] J. H. Lee, S. Natarajan, K. Lee, A model-based predictive control approach to repetitive control of continuous processes with periodic operations, *J. Process Control*, vol. 11, 2001, p 195.

[7] J. H. Lee, M. S. Gelormino, M. Morari, Model predictive control of multi-rate sampled-data systems, *Int. J. of Control*, vol. 55(1), 1991, pp 153-191.

[8] C.V. Rao, S.J. Wright, J.B. Rawlings, Application of Interior-Point Methods to Model Predictive Control, *J. of Optimization Theory and Applications*, vol. 99(3), 1998, pp 723-757.